Bromine-bridged Dy2 single-molecule magnet: magnetic anisotropy driven by cis/trans stereoisomers

Min Li, Haipeng Wu, Zhengqiang Xia, Vincent Montigaud, Olivier Cador, Boris Le Guennic, Hongshan Ke, Wenyuan Wang, Gang Xie, Sanping Chen

Bromine-bridged Dy₂ single-molecule magnet: magnetic anisotropy driven by *cis/trans* stereoisomers

Min Li,‡[a] Haipeng Wu,‡[a] Zhengqiang Xia,*[a] Vincent Montigaud,[b] Olivier Cador,[b] Boris Le Guennic,*[b] Hongshan Ke,[a] Wenyuan Wang,*[a] Gang Xie[a] and Sanping Chen*[a]

[a.] Key Laboratory of Synthetic and Natural Functional Molecule Chemistry of Ministry of Education, College of Chemistry and Materials Science, Northwest University, Xi'an, 710127, China
E-mail: northwindy@126.com, wangwy@nwu.edu.cn, sanpingchen@126.com.

[b.] Univ Rennes, CNRS, ISCR (Institut des Sciences Chimiques de Rennes) –UMR 6226, F-35000 Rennes, France
E-mail: boris.leguennic@univ-rennes1.fr.

We report the first bromine-bridged dinuclear [Dy(Cy₃PO)₂(μ-Br)(Br)₂]₂·2C₇H₈ single-molecule magnet with an effective energy barrier of 684 K and magnetic hysteresis below 3 K. The asymmetric Dy^III centres present two unique stereoisomeric octahedral coordination environments depending on the *cis/trans* disposition of the Cy₃PO ligands, leading to the orthogonality of the easy magnetic axes that annihilate the dipolar interactions.

Recently, research on lanthanide-based single-molecule magnets (SMMs) has made astonishing strides thanks to the increasing knowledge of manipulating the electronic structure of the magnetic centers and some non-traditional ingenious synthetic approaches.[1] Notably, in highly coordinated lanthanide systems, exploiting the symmetry strategy to suppress transverse crystal-field components makes the several complexes entering the club of 1000 K energy barrier.[2] A substantial leap in molecular magnetic hysteresis above the liquid nitrogen temperature (>77 K) have been recently realized by removing equatorial ligands in an organometallic Dy^III metallocenium cation.[3] Inspired by the first generation of SMMs, based on 3*d* transition metals, polynuclear species were also investigated. These systems allow to take advantage of the magnetic interactions to reduce the quantum tunneling of magnetization (QTM).

However, the progress in the development of polynuclear lanthanide-based is relatively slow and the highest relaxation barriers remain in the order of a few hundred Kelvin in some Tb^III and Dy^III dimers.[4] These sophisticated architectures are very appealing since they offer the possibility to conserve the highly anisotropic nature of the individual spins while potentially reducing QTM through appropriate magnetic coupling. The strength of magnetic interactions is highly dependent on the nature of the bridging ligands.[5] Usually, the Ln–Ln interactions are weak and of a few wavenumbers due to the core-like character of 4*f* electrons. Remarkably, the diffused electron cloud distribution of soft ligands, such as the S⁻ and radical bridges, can effectively infiltrate into the 4*f* shell of lanthanide ions which are proved excellent in promoting Ln–Ln interactions.[4c,6] The anisotropy of each monomer controlled by the ligand field remains the key parameter to improve the SMM property since the magnetic relaxation observed for the whole molecule is driven by local single-ion anisotropy.[7] In polymetallic 4*f* block species, the weak interactions between metallic centres, of dipolar and/or exchange origin, are only acting as perturbations on single-ion anisotropy.[8] But manipulating the relative orientations of the local anisotropies to maximize the collective effect for a given size of aggregate is facing severe challenges.[9] In dimers, one should pay attention not to stabilize a non-magnetic ground state due to the antiferromagnetic arrangement of neighbouring magnetic moments. Such arrangement is governed by fundamental geometrical considerations when dipolar terms dominate.[10] To this end, the design of chemical objects with peculiar structural organization between magnetic moments of lanthanide allows the exploration of the subtle balance between single ion anisotropy and magnetic interactions.

Herein we report an extreme organization with the successful assembly of heavy *p*-block bromine-bridged Dy₂ SMM [Dy(Cy₃PO)₂(μ-Br)(Br)₂]₂·2C₇H₈ (**Dy₂**) (Cy₃PO = tricyclohexylphosphine oxide) with orthogonal magnetic moments. Very intriguingly, the metal ions present two unprecedented stereoisomers within a dimer that differ by the *cis/trans* positions of the two Cy₃PO ligands. The octahedron is completed by the additional four weak Br⁻ donors leading to both longitudinally contracted and elongated octahedra. Interestingly, the binuclear asymmetric structure induces dramatically different anisotropies on both Dy^III ions. The *cis/trans* disposition of the Cy₃PO ligands and the presence of the Br⁻ bridges promote the orthogonal arrangement of the anisotropy axes and therefore almost hide the dipolar interaction in the dimer.

Fig. 2 Thermal evolution of the magnetic susceptibility and evolution of the magnetization with applied magnetic field at 2 K (inset) for **Dy₂**. The experimental values are represented as black dots while theoretical data are represented as red lines.
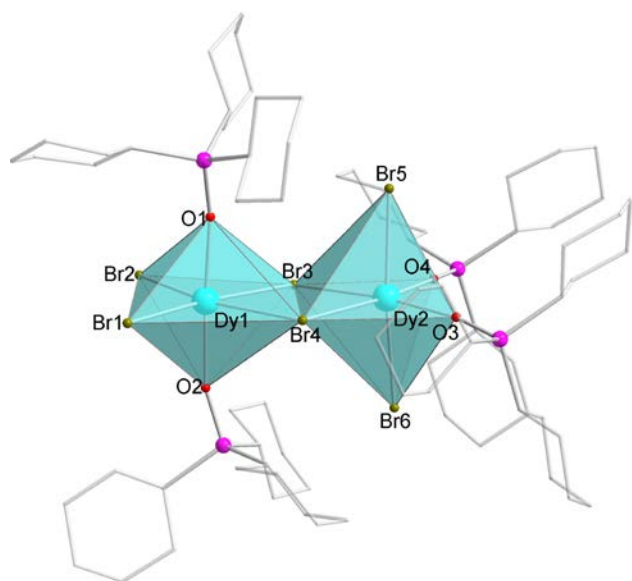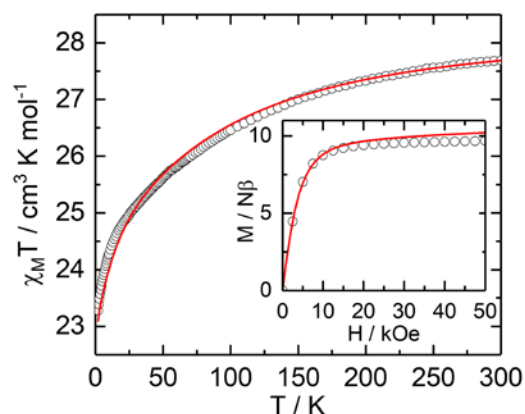
Fig. 1 Structure of **Dy₂** (a) and Dy^{III} coordination polyhedra (b). Solvent molecules and hydrogen atoms have been omitted for clarity.

The addition of DyBr₃ and Cy₃PO at a 1:2 molar ratio in toluene produced white suspension solution in which colorless crystals of **Dy₂** were obtained from the filtered extract in 72% yield. Complex **Dy₂** crystallizes in the triclinic space group $P\bar{1}$ (Table S1) with the asymmetric unit containing two crystallographically independent Dy^{III} ions, four Cy₃PO ligands, six Br⁻ ions and two C₇H₈ solvent molecules. Each Dy^{III} is complexed by four Br⁻ ions and two Cy₃PO ligands creating a distorted octahedral environment (Fig. 1; Table S2).[11] Dy-O distances are considerably shorter than Dy-Br (Table S3): 2.2 Å vs 2.7~2.9 Å. For Dy1, the two *trans* phosphoryl oxygens of the Cy₃PO ligands (O1-Dy1-O2 = 170.84(10)°) provides an apparent pseudo-linear two coordinated environment to the central Dy1 with strong axial LF. Conversely, for Dy2, the two Cy₃PO ligands are in *cis* position transversely coordinated to the tetragonal plane. Dy1 make shorter bonds with terminal Br⁻ than Dy2: $d_{Dy1-Br1}$ = $d_{Dy1-Br2}$ = 2.73 Å while $d_{Dy2-Br5}$ = 2.77 Å and $d_{Dy2-Br6}$ = 2.81 Å. The distances between bridging bromide and metal centres are comprised between 2.87 and 2.95 Å but still longer for Dy1. 4.46 Å separate Dy1 and Dy2 and Dy-Br-Dy angles are 100.128(12)° and 99.684(11)°. The shortest intermolecular Dy···Dy distance is 11.503(5) Å, indicating well-isolated units for **Dy₂** (Fig. S1).

Direct-current (dc) magnetic susceptibility of **Dy₂** and isostructural **Gd₂** were collected at 1 kOe applied field from 2-300 K (Fig. 2 and S2). The room temperature $\chi_M T$ value of 27.7 and 15.71 cm³ K mol⁻¹ is slightly smaller than the theoretical value of 28.34 and 15.76 cm³ K mol⁻¹ for two uncoupled Dy^{III} ($^6H_{15/2}$, S = 5/2, L =5, g_J = 4/3) and Gd^{III} ($^8S_{7/2}$, S = 7/2, L = 0, g_J = 2) ions, respectively. Upon cooling, the $\chi_M T$ profile of **Dy₂** monotonically decreases to 23.3 cm³ K mol⁻¹ at 2 K. However, for **Gd₂**, the $\chi_M T$ value remains constant with decreasing temperature, with a sharp decrease below 50 K to reach minimum value at 2 K. The isothermal magnetization data of **Dy₂** below 5 K reveal a rapid increase at low field and then tends to saturate at 9.7 Nβ at 50 kOe, in agreement with the

presence of two Dy^{III} ions with M_J = ±15/2 (10 Nβ) ground state (Fig. 2, inset and Fig. S3). Simultaneous fitting of the $\chi_M T$ vs T and the M vs H plots with the PHI program[12] leads to J = -0.029 cm⁻¹ with g = 2, thus establishing a weak antiferromagnetic interaction between the Gd^{III} ions (Fig. S2).

The dynamics of the magnetization of **Dy₂** was further studied using alternating-current (ac) susceptibility measurements in zero external dc field. A frequency dependent out-of-phase signal (χ_M'') persists up to 40 K (Fig. 3a and S4). A single relaxation time τ is extracted from frequency-dependent ac signals by a generalized Debye model,[13] giving a narrow relaxation time distribution (α) less than 0.22 (Fig. S5-S6, Table S4). Furthermore, the non-relaxing fraction remains extremely small in the whole temperature range that indicates that the magnetic moments of both sites are involved in the relaxation mechanism and at the same frequency. The application of a magnetic field slows down the

Fig. 3 Frequency-dependent out-of-phase χ_M'' ac susceptibility signals for **Dy₂** at (a) zero and (b) 1000 Oe dc field. (c) Temperature dependence of the relaxation time τ in zero and 1000 Oe dc field for **Dy₂**. The solid lines represent the best fits of the experimental data to multiple relaxation processes. (d) The M vs H hysteresis profiles of **Dy₂** in 2-3 K temperature range, with a magnetic field sweep rate of 8.7 Oe s⁻¹.
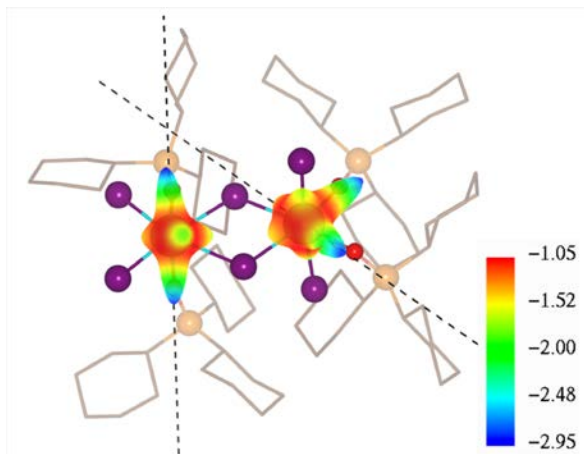
Fig. 4 Representation of the magnetic anisotropy axes and molecular electrostatic potential computed for the ground state KD of each Dy[III] centre, for **Dy₂**.

relaxation processes significantly (Fig. S7). The optimum field at which relaxation is the slowest is estimated at 1000 Oe for which QTM effect is efficiently suppressed. The relaxation is slowed down as shown by a shift in the maxima of χ_M'' to lower frequencies (Fig. 3b and S8-S9). The temperature variation of the relaxation time in zero field can be fitted with contributions from QTM, Raman and Orbach processes with eq. 1 (Fig. 3c) provides the resulting parameters U_{eff} = 684.1 K (475.7 cm^{-1}), τ_0 = 3.84 × 10^{-12} s, C = 0.85 s^{-1} K$^{-2.55}$, n = 2.55 and τ_{QTM} = 1.69 ms.

$$\tau^{-1} = \tau_{QTM}^{-1} + CT^n + \tau_0^{-1}\exp\left(-\frac{U_{eff}}{T}\right) \qquad (1)$$

Fitting the relaxation time at 1000 Oe with the same eq. 1 without QTM gives a slightly greater U_{eff} of 728.3 K (506.5 cm^{-1}) with τ_0 = 2.73 ×10^{-12} s and C = 0.038 s^{-1} K$^{-3.34}$, n = 3.34 (Fig. 3c, Table S5). The slight differences observed between fitted values may be ascribed to the existence of sizable interactions between the magnetic sites.

As another sign of the slow relaxation, magnetic hysteresis of the magnetization was measured for **Dy₂** at a sweep rate of 8.7 Oe·s^{-1} (Fig. 3d). Butterfly-shaped hysteresis loops closing at zero field and slightly opening at higher field were observed up to 3 K. This is consistent with the magnetic relaxation times obtained from ac susceptibility data and the presence of quantum tunnelling at zero dc field.

Ab initio SA-CAS(9,7)SCF/RASSI-SO/SINGLE_ANISO calculations are performed for each inequivalent Dy[III] centre to rationalize the magnetic and electronic properties of **Dy₂** (see Supporting Information for details). The calculated eight lowest KDs and local *g* tensors highlight different behaviours for the two Dy[III] sites. In the case of Dy1 (coordinated to the two *trans* Cy₃PO ligands), a pure M_J = ±15/2 ground state characterized by an Ising-type magnetic anisotropy axis (g_Z = 19.87 and $g_X = g_Y$ = 0.00) is observed (Table S6). The anisotropy axis is along the most negatively charged axial Cy₃PO ligands, almost perpendicular (89°) to the tetragonal bromine plane (Fig. 4). This axial repartition of the electronic density around the Dy[III] ion leads to a large splitting of the $^6H_{15/2}$ ground multiplet spanning over 800 cm^{-1}. For Dy2, the *cis* disposition of the Cy₃PO ligands lowers the anisotropy character of the *g*-

tensor (g_X = 0.06, g_Y = 0.75 and g_Z = 18.70) reflecting a less pure ground state (90% M_J = ±15/2, Table S7) and a smaller splitting of the $^6H_{15/2}$ ground multiplet (around 350 cm^{-1}). The orientation of the magnetic axis still remains along one of the *cis* Cy₃PO moieties, in the tetragonal plane (Fig. 4). These orientations are further supported by the representation of the total molecular electrostatic potential mapped around each Dy[III] ion using home-made CAMMEL program (details in the SI).[14] These results on isolated magnetic centres highlight the influence of the coordination polyhedron on the stabilization of the highly anisotropic M_J = ±15/2 ground state.

In order to give a more complete description of the magnetic properties, the magnetic interactions occurring in **Dy₂** are then considered in the calculations. According to crystallographic data, the intermolecular interactions are neglected due to the large Dy···Dy distances and only intramolecular interactions are taken into account. The magnetic coupling in **Dy₂** was estimated by considering dipolar and exchange terms within the Lines model, with an effective spin 1/2 (eq. 2), as implemented in the POLY_ANISO routine.[15]

$$\widehat{H_{ex}} = -J^{dip}\widetilde{S_1}\widetilde{S_2} - J^{ex}\widetilde{S_1}\widetilde{S_2} \qquad (2)$$

First, the intramolecular dipolar interactions are calculated following eq. 3.

$$E = \frac{\mu_0}{4\pi r^3}\left[\mu_1 \cdot \mu_2 - \frac{3}{r^2}(\mu_1 \cdot r)(\mu_2 \cdot r)\right] \qquad (3)$$

with μ_1, μ_2 being the magnetic moment vectors of Dy1 and Dy2 respectively, and r being the Dy1-Dy2 vector. The dipolar term therefore depends on both the distance and the orientation of the anisotropy axes. Since the two anisotropy vectors are almost orthogonal (89°), a very low value of the dipolar term is expected. Indeed, the computed dipolar term is -0.13 cm^{-1} leading to the energy splitting observed in Table S8. Then, to complement the qualitative picture of the intramolecular interactions, the effective exchange parameter J^{ex} is fitted
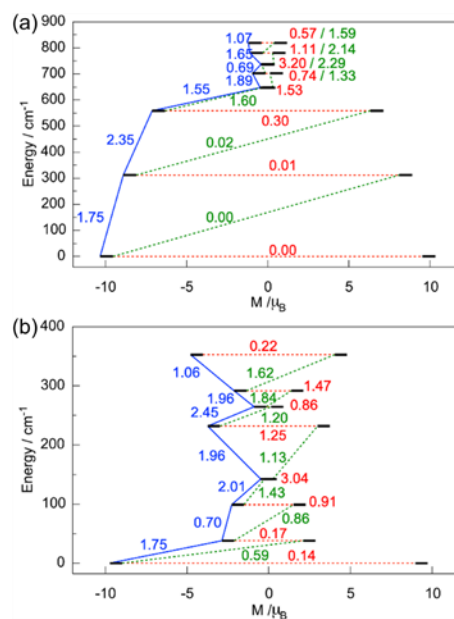

Fig. 5 *Ab initio* computed magnetization blocking barrier for Dy1 (a) and Dy2 (b). The dotted green and blue lines show possible Orbach processes, dotted red lines quantum tunnelling processes.

according to the experimental data. The best agreement is found for J^{ex} = -0.79 cm^{-1} leading to the exchange spectrum in Table S8. The computed dc magnetic properties are represented in Fig. 2. Superexchange interactions through bromide bridges override dipolar coupling because of the orthogonality between the easy magnetic axes, a spectacular effect of the peculiar *cis/trans* topology in the dimer.

The calculated transition magnetic moment elements, obtained from the *ab initio* single-ion analysis, are depicted in Fig. 5. Let us mention that this interpretation does not directly take into account hyperfine interactions[16] and spin-phonon couplings.[17] For Dy1, the ground and first excited state QTM components are found to be negligible (0-10^{-2} μ_B) and a significant magnetic axiality is still maintained in the 2nd excited state. Therefore, the most probable relaxation pathway involves the third excited state with an energy barrier of approx. 600 cm^{-1}, slightly higher than the experimental data (about 500 cm^{-1}). On the contrary, a faster relaxation pathway is predicted for Dy2. The calculated transverse transition matrix element between the ground state KD is already large (0.14 μ_B), promoting a faster QTM compared to Dy1. While experimentally we cannot discriminate the two Dy^{III} sites (one single relaxation), the calculations evidence the presence of two drastically different magnetic centres: i) a strongly anisotropic one (Dy1) with the two *trans* Cy$_3$PO ligands; ii) Dy2, with the LF dictated by the *cis* configuration of the Cy$_3$PO ligands, inducing a lower magnetic anisotropy character and a faster relaxation mechanism.

In summary, the first bromine-bridged octahedral dinuclear Dy^{III} SMM has been synthesized and characterized. The complex presents a stereoisomeric dimer system with drastically different local anisotropies. Superexchange interactions through bromide bridges override dipolar coupling because of the orthogonality between the easy magnetic axes. Calculations suggest that the observed magnetic relaxation is dominated by the strong axial anisotropy of one dysprosium centre. The second dysprosium ion, with an almost planar anisotropy, is monitored through superexchange interaction. Polymetallic lanthanide systems based on asymmetric building blocks with perpendicular anisotropy arrangements still offer a playground for investigation of relaxation mechanisms in lanthanide SMMs.

Conflicts of interest

There are no conflicts to declare.

Notes and references

1   (a) F. S. Guo, A. K. Bar and R. A. Layfield, *Chem. Rev.*, 2019, **119**, 8479-8505; (b) J. L. Liu, Y. C. Chen and M. L. Tong, *Chem. Soc. Rev.*, 2018, **47**, 2431-2453; (c) J. D. Rinehart and J. R. Long, *Chem. Sci.*, 2011, **2**, 2078-2085; (d) B. M. Day, F. S. Guo and R. A. Layfield, *Acc. Chem. Res.*, 2018, **51**, 1880-1889.

2   (a) J. Liu, Y. C. Chen, J. L. Liu, V. Vieru, L. Ungur, J. H. Jia, L. F. Chibotaru, Y. Lan, W. Wernsdorfer, S. Gao, X. M. Chen and M. L. Tong, *J. Am. Chem. Soc.*, 2016, **138**, 5441-5450; (b) Y.S. Ding, N. F. Chilton, R. E. P. Winpenny and Y.Z. Zheng, *Angew. Chem. Int. Ed.*, 2016, **55**, 16071-16074; (c) A. B. Canaj, S. Dey, E. R. Martí, C. Wilson, G. Rajaraman and M. Murrie, *Angew. Chem. Int. Ed.*, 2019, DOI: 10.1002/anie.201907686.

3   F.-S. Guo, B. M. Day, Y. C. Chen, M. L. Tong, A. Mansikkamäki and R. A. Layfield, *Science,* 2018*,* **362***,* 1400-1403

4   (a) J. Xiong, H. Y. Ding, Y. S. Meng, C. Gao, X. J. Zhang, Z.-S. Meng, Y. Q. Zhang, W. Shi, B.-W. Wang and S. Gao, *Chem. Sci.*, 2017, **8**, 1288-1294; (b) F. Liu, G. Velkos, D. S. Krylov, L. Spree, M. Zalibera, R. Ray, N. A. Samoylova, C. H. Chen, M. Rosenkranz, S. Schiemenz, F. Ziegs, K. Nenkov, A. Kostanyan, T. Greber, A. U. B. Wolter, M. Richter, B. Büchner, S. M. Avdoshenko and A. A. Popov, *Nat. Commun.*, 2019, **10**, 571; (c) S. Demir, M. I. Gonzalez, L. E. Darago, W. J. Evans and J. R. Long, *Nat. Commun.*, 2017, **8**, 2144.

5   S. Goswami, A. K. Mondal and S. Konar, *Inorg. Chem. Front.*, 2015, **2**, 687-712.

6   (a) F. Tuna, C. A. Smith, M. Bodensteiner, L. Ungur, L. F. Chibotaru, E. J. McInnes, R. E. Winpenny, D. Collison and R. A. Layfield, *Angew. Chem. Int. Ed.*, 2012, **51**, 6976-6980; (b) J. D. Rinehart, M. Fang, W. J. Evans and J. R. Long, *J. Am. Chem. Soc.*, 2011, **133**, 14236-14239.

7   D. Gatteschi, R. Sessoli and L. Sorace, *Handbook on the Physics and Chemistry of Rare Earths*, J.-C. G. Bünzli and V. K. Pecharsky, Elsevier, 2016, **50**, 91-139.

8   L. F. Chibotaru, Theoretical understanding of Anisotropy in Molecular Nanomagnets. In Gao, S. (ed.) Molecular Nanomagnets and Related Phenomena vol. **164** of Struct. Bond. 185-229, Springer Berlin Heidelberg, 2015.

9   (a) R. Ruamps, R. Maurice, C. de Graaf and N. Guihéry, *Inorg.Chem.*, 2014, **53**, 4508-4516; (c) E. Moreno Pineda, N. F. Chilton, R. Marx, M. Dorfel, D. O. Sells, P. Neugebauer, S. D. Jiang, D. Collison, J. van Slageren, E. J. McInnes and R. E. Winpenny, *Nat. Commun.*, 2014, **5**, 5243.

10 L. Ungur, S.-Y. Lin, J. Tang and L. F. Chibotaru, *Chem. Soc. Rev.*, 2014, **43**, 6894-6905.

11 M. Llunell, D. Casanova, J. Cirera, Alemany and P. Alvarez, SHAPE (2.1), Barcelona, Spain, 2013.

12 N. F. Chilton, R. P. Anderson, L. D. Turner, A. Soncini and K. S. Murray, *J. Comput. Chem.*, 2013, **34**, 1164-1175.

13 D. Gatteschi, R. Sessoli and J. Villain, *Molecular Nanomagnets, Oxford University Press, Oxford*, 2006.

14 (a) K. Zhang, V. Montigaud, O. Cador, G. P. Li, B. Le Guennic, J. K. Tang and Y. Y. Wang, *Inorg. Chem.*, 2018, **57**, 8550-8557; (b) G. Huang, G. Fernandez-Garcia, I. Badiane, M. Camarra, S. Freslon, O. Guillou, C. Daiguebonne, F. Totti, O. Cador, T. Guizouarn, B. Le Guennic and K. Bernot, *Chem.-Eur. J.*, 2018, **24**, 6983-6991.

15 (a) L. F. Chibotaru, L. Ungur and A. Soncini, *Angew Chem Int Ed*, 2008, **47**, 4126-4129; (b) L. Ungur, W. Van den Heuvel and L. F. Chibotaru, *New J. Chem.*, 2009, **33**, 1224-1230.

16 F. Pointillart, K. Bernot, S. Golhen, B. Le Guennic, T. Guizouarn, L. Ouahab and O. Cador, *Angew. Chem. Int. Ed.*, 2015, **54**, 1504-1507.

17 (a) L. Escalera-Moreno, N. Suaud, A. Gaita-Ariño and E. Coronado, *J. Phys. Chem. Lett.*, 2017, **8**, 1695-1700; (b) A. Lunghi, F. Totti, S. Sanvito and R. Sessoli, *Chem. Sci.*, 2017, **8**, 6051-6059; (c) A. Lunghi, F. Totti, R. Sessoli and S. Sanvito, *Nat. Commun.*, 2017, **8**, 14620; (d) C. A. P. Goodwin, F. Ortu, D. Reta, N. F. Chilton and D. P. Mills, *Nature*, 2017, **548**, 439-442.